Single trial characterization of frontal Theta and parietal Alpha oscillatory episodes during Spatial Navigation in humans

KEYWORDS:

Spatial navigation, brain oscillations, theta, alpha, virtual reality, electroencephalography

ABSTRACT:

Theoretical proposals and empirical findings both highlight the relevance of Theta brain oscillations in human Spatial Navigation. However, whilst the general assumption is that the relevant Theta band activity is purely oscillatory, most empirical studies fail to disentangle oscillatory episodes from wide band activity. In addition, experimental approaches often rely on averaged activity across trials and subjects, disregarding moment-to-moment fluctuations in Theta activity, contingent on key aspects of the task. Here, we used novel oscillation detection approaches to investigate the dynamics of Theta and Alpha episodes in human subjects performing a Spatial Navigation task, resolved at single trial level. The results suggest that bouts of Theta oscillatory activity are related to task difficulty and access to previously encoded information, across different time-scales. Alpha episodes, instead, seem to anticipate successful navigational decisions and could be related to shifts in internal attention.

INTRODUCTION

Spatial Navigation (SN), an essential skill for many animal species including humans, is a complex ability that draws on multiple basic cognitive processes, such as memory, attention, proprioception, executive control, and decision making (Do et al., 2021). SN capacity tends to decline with age, leading to a loss of autonomy and life quality in the elderly (Burns, 1999). Furthermore, topographical disorientation characterizes some age-related conditions such as MCI and AD, and has been suggested as a potential biomarker of cognitive decline (Plácido et al., 2022). Due to its relevance, the cognitive and physiological bases of SN have been thoroughly investigated in non-human (Buzsáki, 2005; O'Keefe & Conway, 1978) and human animals (Epstein et al., 2017). However, whereas animal research and invasive methods in humans have highlighted the great relevance of episodes of oscillatory neural activity on a single-trial basis, non-invasive human research has been more limited in this respect. Here, we build on recent advances in oscillation detection methods to characterise oscillatory episodes on human neural activity during navigation of learnt paths in a virtual reality environment, using scalp EEG.

Electrophysiological studies of SN in rodents have revealed the importance of hippocampal Theta (3 to 8 Hz) oscillatory episodes, thought to help organize spatial information into cognitive maps that allow to integrate external information for flexible behaviour (O'Keefe & Nadel, 1978). More recent proposals have suggested that the role of the hippocampus is, more generally, to organize external cues into cognitive maps that can be accessed through memory. That is, cognitive maps include, but are not restricted to, spatial representations (Buzsáki, 2005; Eichenbaum, 2017; Epstein et al., 2017), an interpretation that harkens back to the concept of cognitive map originally introduced by Tolman (1948).

In humans, "pen-and-paper" tests of SN (Cogné et al., 2017) have given way to the use of Virtual Reality (VR). VR environments can produce close-to-realistic immersive experiences whilst allowing for experimental control (Diersch & Wolbers, 2019). Furthermore, VR has been proposed as a valuable tool for assessing navigational disorders and as a potential device for interventions (Cogné et al., 2017), given that SN performance in VR environments and in real life are highly correlated (Cushman et al., 2008; Diersch & Wolbers, 2019). For example, age-related decline in SN skills in VR tasks seems to be comparable to real life (Cushman et al., 2008).

Non-invasive neuroimaging during SN in VR environments allows for the evaluation of neural correlates in humans during realistic navigation tasks, enabling the analysis of increasingly sophisticated patterns using oscillatory episode modelling (Caplan et al., 2001), source localization (Bauer et al., 2021), and multivariate analysis (Do et al., 2020; Zhu et al., 2022). Tasks like the Morris water maze (Thornberry et al., 2023), T-junction mazes (Bischof & Boulanger, 2003; Caplan et al., 2001), navigation through virtual cities (Araújo et al., 2002; Bischof & Boulanger, 2003) or real environments (Zhu et al., 2022) are some of the scenarios used in the study of human SN. At present, rich datasets and knowledge from neuroimaging studies make it possible to investigate, at single trial level, neural dynamics in relation to the instantaneous navigational state. Given that the brain operates through online computations, it is important to address relevant information contained in moment-to-moment variability as opposed to averages. For instance single-trial analysis of phase precession showed that the phase span of precession is reduced when single-trial is analysed compared to pooled data (Schmidt et al., 2009).

One the other hand, invasive approaches using intracranial recordings of electrophysiological activity have allowed to link hippocampal Theta to SN in humans, similar to what was found earlier in other animal models (Bohbot et al., 2017; Ekstrom et al., 2005). In addition, fMRI and invasive electrophysiological studies suggest that an extended network of brain areas is involved in SN, including, but not limited to the hippocampus, parietal cortex and prefrontal cortex (Baumann & Mattingley, 2021; Caplan et al., 2001; Ekstrom et al., 2017; Hyman et al., 2005; Kahana et al., 1999; Patai & Spiers, 2021). Some of these studies show that it is possible to extract SN-related electrophysiological activity from scalp electroencephalography (EEG), which allows subjects to move freely, bringing the study of SN closer to near-realistic scenarios. These EEG studies have predominantly highlighted the relevance of oscillatory frequencies in the Theta range (3-8 Hz) and, to a lesser extent, in Alpha (8-14 Hz).

The amplitude of Theta oscillations (commonly observed in frontal areas in non-invasive electrophysiological recordings), has been reported to increase during movement compared to standing still (Liang et al., 2018), during navigation compared to non-navigation periods (Araújo et al., 2002), in difficult compared to easy navigation SN tasks (Caplan et al., 2001; Kahana et al., 1999), during free exploration compared to guided navigation (Chrastil et al., 2022), when subjects approach a target (Bauer et al., 2021), collide with (invisible) walls in virtual mazes (Gehrke & Gramann, 2021), must re-calculate paths(Do et al., 2021), and after a navigational decision (Bischof & Boulanger, 2003). Some studies have reported increased Theta activity specifically after a successful navigational decision (Bauer et al., 2021; Chrastil et al., 2022; White et al., 2012), although not all studies have observed this correlation (Caplan et al., 2001). In summary, many studies report increases in Theta oscillations during relevant SN events (whilst some other studies have also reported decreases in Theta activity, associated with spatial learning (Thornberry et al., 2023)).

In addition to Theta, non-invasive electrophysiological studies in humans have found correlates between SN and Alpha oscillatory activity (8 to 14 Hz). Usually, Alpha oscillatory activity is observed in parietal and occipital areas and, it has been reported to increase or decrease in different contexts. For example, Alpha desynchronization has been suggested to reflect switches between allocentric and egocentric reference frames(Do et al., 2021). Processing of SN-relevant sensory information also results in Alpha decreases, after collision with invisible obstacles (Gehrke & Gramann, 2021) or during navigation compared to non-navigation epochs (Araújo et al., 2002). However, some authors link posterior Alpha desynchronization with visual flow, rather than specifically with SN operations (Liang et al., 2018). Though less frequently reported, increases in Alpha activity have also been observed, such as in free compared to guided navigation (Chrastil et al., 2022), or when walking away from invisible boundaries in a virtual maze (Gehrke & Gramann, 2021).

According to the studies briefly discussed above, there is evidence of the involvement of Theta and Alpha oscillations in various aspects of SN, such as path difficulty, familiarity, encoding success, or navigation strategy. Yet, their specific role is far from clear. First, most of these past

studies focus on average activity across subjects and/or trials, therefore disregarding moment-to-moment online modulations of Theta/Alpha activity at different stages of the task (though see, (Gehrke & Gramann, 2021; Zhu et al., 2022), for exceptions). This is particularly relevant given the importance of trial-level modulations in animal research, and the effort that researchers put into measuring SN using realistic (and therefore complex) navigation paradigms. It is, therefore, crucial to evaluate the data with analytic approaches that allow addressing the neural correlates of navigation to a finer level of detail. Second, despite many SN theories attribute significance to the oscillatory nature of Theta activity, it is not always clear whether the neural activity observed is really oscillatory. It is fundamental to disentangle transient episodes of oscillatory activity from background, aperiodic, neural activity (referred sometimes as background 1/f activity), as they are usually conflated in the EEG signal (Gerster et al., 2022). Conventional time-frequency methods based on trial-averages fail at this, as differences in the power of a certain frequency band can be due not only to differences in oscillatory activity but also in background activity (Donoghue et al., 2022), and estimates of peak (dominant) frequency can be strongly biased by aperiodic activity (Samaha & Cohen, 2022).

Recent advances, based on the Better Oscillation detection method (BOSC) originally developed by Caplan et al. (2001) for intracranial EEG, allow now for the extraction of oscillatory episodes in scalp EEG data (Du et al., 2023; Gehrke & Gramann, 2021). As they allow to extract time-resolved, single trial information of purely oscillatory activity, this approach is optimal to address transient episodes of oscillatory activity during SN in non-invasive data. So far, prior studies that have focused on oscillatory episodes either with invasive or non-invasive EEG (Caplan et al., 2001; Du et al., 2023; Gehrke & Gramann, 2021; Kahana et al., 1999), relied on simplified designs to satisfy a specific hypothesis-driven question (for instance, long vs. short mazes or correct vs. incorrect decisions). In the present study, we have adopted a hypothesis-free approach, based on estimating the abundance of Theta and Alpha oscillatory episodes at single trial level as humans navigate through a realistic virtual environment. We aim to understand how these oscillatory episodes emerge online as a function of variations in specific properties of the trial such as familiarity with the path, location within the path, distance to the next turn, and accuracy.

RESULTS

Behavioural results

Subjects learnt five 10-junction mazes in a virtual environment, driving a car through a simulated cityscape. After an initial guided run of each maze, participants had three attempts (runs) to navigate the learnt path in an Immediate recall task, each run terminating when the maze was completed or when a mistake was made. After a break that included a distraction task, subjects had 5 more attempts at completing the learnt mazes in a Delayed recall task (see Methods for full details).

All subjects reached the end of all Guided mazes. Most subjects (N=20) required only one attempt in all 5 mazes, 3 subjects committed an error in 1 out of the 5 mazes, and 1 subject committed an error in 2 runs of one of the 5 mazes. On average, subjects correctly recalled 8.31±1.15 (average ± SD) junctions in the Immediate recall mazes and 5.95±1.71 in the Delayed recall mazes. In both cases, the number of consecutive correct junctions increased with each run (Figure 1).

Oscillatory episodes

We used an oscillation detection method to estimate the abundance of oscillatory episodes in the relevant frequencies and scalp locations (see Methods for details on the analytical pipeline, and statistical approach). At group level, most of the oscillatory episodes (Figure 2F) were observed at frequencies below 15 Hz (Figure 2A). The abundance of Theta (3 to 8 Hz) episodes during the SN task was higher in frontal channels, with the maximum at electrode Fz (Figure 2B). Both the power spectrum of the channel and abundance of oscillatory episodes displayed a double peak, with the maximum in the Theta range, at 6.5 Hz, and a lower peak in the Alpha

range, at 9 Hz (Figures 2D and Supplementary Figure S2A). Mean Theta abundance was 20±12%, and the episodes had a mean duration of 5±1 cycles (880±140 ms). By contrast, the power spectrum and abundance of channel Fz at rest presented a clear single peak at 9 Hz (Figure 2E and Supplementary Figure S2B). The abundance of Theta episodes in channel Fz at rest was 14±9%, significantly lower than during the task (two-tail paired t-test, alpha level 0.05, t(23)= -2.9167, p-value=0.008, Cohen's d=-0.6).

Alpha (8.5 to 14 Hz) episodes were more abundant over parietal areas, with the maximum at electrode Pz (Figure 2C). The power spectrum and the abundance of oscillatory episodes displayed a single peak in the Alpha range, at 9 Hz (Figure 2D and Supplementary Figure S2A). Mean Alpha abundance was 15±10%, Alpha mean episode duration was 5±1 cycles (480±90 ms). At rest, both power spectrum and Alpha abundance at channel Pz presented a clear single peak at 9 Hz (Figure 2E and Supplementary Figure S2B). The abundance of Alpha episodes during rest (46±20%) was significantly higher than during the task (two-tail paired t-test, alpha level 0.05, t(23)= 6.3446, p-value=$2 \cdot 10^{-6}$, Cohen's d=1.3).

The abundance of oscillatory episodes was highly variable between subjects for both Theta and Alpha bands (Figure 3). There was no correlation between Theta and Alpha abundance across subjects (r=0.017, p-value=0.93).

Theta episodes were more abundant in Delayed recall mazes, compared to Immediate recall mazes (Figure 4A-E). Episode abundance increased with run number (Figure 4A), and it was larger in the central junctions of a given maze, specially at early times within the approach to the junction (Figure 4B, Figure 4C and Figure 5). Correct decisions resulted in decreased Theta episode abundance, only for Immediate recall mazes (Figure 4D). Finally, Theta abundance did not differ for solved and unsolved mazes (Figure 4E).

Contrary to Theta episodes, the abundance of Alpha episodes did not seem to strongly differ between the Immediate and Delayed recall stages (Figures 4F-J and 6). Alpha episodes increased monotonically during the first 4 runs (Figure 4F) and were more abundant in the first junctions of the mazes, specially at the early time segments within the junction (Figure 4G, Figure 4H and Figure 6). Successful navigational decisions were preceded by increased Alpha abundance at junction level (correct compared to incorrect decisions, Figure 4I) as well as at maze level (solved compared to unsolved mazes, Figure 4J).

Statistical analysis

For the Theta band, electrode Fz, the model that best described the data was (See Supplementary Materials, 2.2. Model selection):

$$Abundance \sim Stage + Run + Junction + \mathrm{Time} + (1|Participant)$$

Stage, Junction and Time had a significant impact on Theta Abundance (Supplementary Table S3, Figure 7), whereas Run, Correct response and Solved did not had an impact on Theta Abundance. Post-hoc tests (Supplementary Table 3) indicated that Abundance was significantly higher in the Delayed recall mazes compared to Immediate recall mazes, in the middle of the maze (Junctions 5 and 6) compared to the beginning or end of the maze (Junctions 1 and 10), and at the early times of the trial compared to medium and late times. Interestingly, these effects were mostly driven by Delayed recall trials (Supplementary materials and methods: 3.3. Models for Immediate recall and Delayed recall trials) whereas in Immediate recall trials only the response (Correct or Incorrect) had an impact on oscillatory Theta episodes.

For the Alpha band at electrode Pz, the model that best described the data was (See Supplementary Materials, 2.2 Model selection):

$$Abundance \sim Stage + Junction + \mathrm{Time} + Correct + (1|Participant)$$

Abundance in the Alpha range was modulated by Stage, Junction, Time and Turn accuracy (Correct) (Supplementary Table S4, Figure 8), whereas Run and Solving the maze had no impact on Alpha abundance. Post-hoc tests (Supplementary Table S9) revealed an increase in

Alpha episodes during Delayed recall mazes compared to Immediate recall mazes, as in the middle Junctions of the maze (Junctions 3 and 4) compared to the first Junction. We also observed a decrease in abundance of Alpha oscillatory episodes as the subject approached the decision point within a trial. Finally, Alpha abundance was higher in trials where subject made a Correct turn decision, compared to Incorrect decision trials. When we modelled separately Immediate and Delayed recall trials, the pattern of results was similar to the one observed for all trials (Supplementary materials and methods: 3.3 Models for Immediate recall and Delayed recall trials.).

Summarizing, both frontal Theta and parietal Alpha oscillatory episode abundance increased during Delayed recall compared to Immediate maze recall. In addition, although for both frequency bands abundance increased as subjects advanced through the sequence of junctions along a maze, Alpha episode abundance peaked before to Theta abundance (Figure 8), and only Theta abundance decreased significantly by the end of the maze (Figure 8). In addition, parietal Alpha oscillatory episodes abundance differed as a function of upcoming turn accuracy, with abundance being higher before correct compared to incorrect turns (Figure 8). Finally, neither the model for Theta nor Alpha bands revealed significant interactions between the factors included in the selected models (See Supplementary Materials and Methods 3.4 Interactions).

DISCUSSION

The present results bring to light the relevance of moment-to-moment episodes of oscillatory neural activity during spatial navigation (SN) in humans, at a single-trial level. The relevance of individual bouts of theta activity has been widely assumed in the literature, but rarely addressed, especially using non-invasive methods. Interestingly, we observed a clear spatial differentiation between the loci of most abundant Theta and Alpha episodes: Theta abundance peaked at frontal locations, whereas Alpha abundance was maximal in parietal sites. The occurrence episodes of frontal Theta and parietal Alpha oscillatory activity was found to be tightly related to relevant events during navigation. We observed differences in the dynamics of the episode abundance both at the long- (along the progressive junctions of the maze)- and at the short time scales (along the path toward a junction within the maze). We observed increases in Alpha episodes at early junctions along the maze, whereas Theta abundance was highest in the middle junctions. Within a single junction arm, Theta episodes were most abundant early on and decreased monotonically as subjects approached the turning point, whereas Alpha episodes sustained throughout the arm's length and decreased only close to the turn. Finally, only Alpha activity correlated with successful navigational decisions: increased abundance of Alpha oscillatory episodes anticipated correct turns.

More generally, our findings also reinforce current views considering that SN is supported by an extended network of brain areas. Although it is probably biased by the vast and important literature using electrophysiology in rodent models, traditional theories consider the Hippocampus to be the key structure in SN (O'Keefe & Nadel, 1978). This view is, at least in part, currently being challenged by newer theories. First, these new theories tend to attribute a more general role to the Hippocampus, which would serve to create cognitive maps, including but not restricted to, SN (Buzsáki & Moser, 2013). Second, although reserving a prominent role to Hippocampal activity, these theories have revealed a wide network of brain areas involved in the computations necessary for SN (Ekstrom et al., 2017). This latter view is supported by neuroimaging studies indicating that oscillatory activity at different frequency bands (Caplan et al., 2001; Chrastil et al., 2022; Jacobs et al., 2010; White et al., 2012; Zhu et al., 2022) and locations (Baumann & Mattingley, 2021; Caplan et al., 2001; Epstein et al., 2017) is involved in SN, including our study, in which both frontal Theta and parietal Alpha varied as a function of different aspects of the SN task.

In our study, frontal Theta abundance was related to global properties of the navigation task. At the longest time-scale tested, we observed increased abundance of Theta episodes during Delayed Recall compared to Immediate Recall, in agreement with the seminal findings of Kahana et al. (1999) using intra-cranial recordings in humans. This increase of Theta episodes

could be explained by an anticipation of the properties of the task: Theta episodes are more abundant in the more difficult Delayed Recall mazes, possibly revealing the effortful retrieval of previously encoded paths. At a shorter time-scale, involving the junction-to-junction sequence within a maze, Theta abundance was observed to increase precisely in the middle junctions. A feasible interpretation of this result aligns with the classical serial position effect in memory for sequences, a phenomenon that has been also reported to apply in the context of SN (Hilton et al., 2023). In short, T-Junction mazes can be conceptualized as an ordered sequence of binary decisions (for instance LRRLRLLLRR). According to the serial position effect, there would be a facilitation in the encoding and subsequent recall of first and last items of the sequence (due to primacy and recency effects respectively) compared to the middle parts of the sequences. Therefore, in our experiment, increased Theta abundance in the middle part of the mazes can be linked to the increased difficulty of retrieval of these middle junctions (Caplan et al., 2001; Kahana et al., 1999). At the shortest time scale, as the participant progressed toward a junction turn, we observed an initial heightened abundance of Theta episodes followed by a monotonic decrease. This might suggest that subjects accessed encoded path information at early moments in the junction and, once a navigational decision was made, encoded information was not further accessed.

Although previous non-invasive EEG studies have observed a positive correlation between Theta-band activity and performance in SN tasks (Bauer et al., 2021; Chrastil et al., 2022; White et al., 2012), we found that abundance of Theta episodes was not significantly different prior to correct and incorrect navigational decisions, in line with previous studies (Caplan et al., 2001). A possible explanation for the discrepancy can be differences in the SN task: in the studies finding a positive correlation between Theta and SN performance the navigational choices for the subjects were less limited than in our study, where subjects had to choose between only two options. Therefore, the sample of correct responses in our study probably contains trials in which subjects chose the correct decision by chance, possibly blurring the comparison between correct and incorrect choices.

Contrary to Theta, the abundance of Alpha episodes correlated with successful navigational decisions: increased parietal Alpha abundance was found in trials preceding a correct decision. At present, Alpha activity is considered to reflect active inhibition of task-irrelevant representations, such as distractor information (Klimesch, 2012): consistent findings from working memory studies using sequences of simple stimuli (such as letters and numerals) indicate an increase of Alpha power during the retention interval especially when distractor information must be suppressed, and a positive correlation between Alpha power and working memory load (Jensen, 2024). Following these results, Alpha activity has been proposed to protect memory maintenance against distracting information (Bonnefond & Jensen, 2012). The pattern of Alpha episodes in our study would be compatible with this protective role. In line with this idea, increased posterior Alpha oscillations has been suggested to signal switches between internal and external attention (Benedek et al., 2014; Magosso et al., 2021). Interestingly, this has been confirmed also in VR immersive tasks (Magosso et al., 2019). This interpretation aligns well with our results: considering the absence of relevant landmarks inside the mazes, participants had to rely on episodic memory traces. Therefore, increased Alpha abundance in correct decision trials could indicate trials in which subjects managed to focus on internal attention more successfully. Increases in Alpha episode abundance in Delayed Recall compared to Immediate Recall trials could also be explained similarly: in the second stage of the experiment, accessing internal representation of the previously learnt paths was the optimal strategy to solve old mazes. Therefore, Alpha increase in sensory areas would indicate suppression of incoming information possibly distracting from access to internal representations.

It could be argued that the design of our experiment conflates Delayed vs. Immediate Recall with total time on task, complicating the interpretation of variations in Theta and Alpha abundance across experimental stages. Increases in overall Alpha and Theta with time on task have been previously associated with fatigue, drowsiness and task detachment (see Tran et al. (2020) for a systematic review). However, when discussing time-in-task effects, it is important to

dissociate task-related Theta from task-unrelated Theta activity. Arnau et al.(2021) reported that whilst inter-trial Theta activity increased with time on task, task-related activity was reduced; therefore, fatigue and detachment from the task is in fact associated with reduced Theta, an interpretation that aligns with models relating Theta oscillations to cognitive control (Cavanagh & Frank, 2014). Moreover, it is important to note that, in the present experiment, performance did not decrease with time on task (see Supplementary Materials), ruling out a time-dependent task disengagement effect. Therefore, although we cannot completely rule out a contribution of time-on-task, evidence suggests that the increased difficulty (and higher demand on memory) is the most likely explanation for the increase in Theta abundance for Delayed Recall mazes.

One important aspect of the current study is that we used estimations of purely oscillatory activity from the EEG signal, and therefore the abundance data is not contaminated by changes in wide-band activity. It is now accepted that brain oscillatory activity emerges in short intermittent episodes distributed stochastically in time, and with variable duration in cycles, superimposed on the background wide-band aperiodic activity (Jones, 2016; Seymour et al., 2022). Targeting these oscillatory episodes in a time resolved fashion (e.g., at single-trial level) is therefore essential to capture the relationship between neural oscillations and behaviour. Yet, despite its paramount importance, the distinction between oscillatory and aperiodic activity is often neglected (Gerster et al., 2022). Although prevalent theories relating Theta to SN assume that Theta activity involved in information organization and transmission is an oscillation (Buzsáki, 2005; Ekstrom et al., 2017), many electrophysiological studies of SN do not isolate purely oscillatory activity from aperiodic activity, making it impossible to discriminate changes related to oscillatory activity from changes related to broadband activity, that has been shown to vary with task (Gilden, 2001; Ouyang et al., 2020; Podvalny et al., 2015; Waschke et al., 2021). Our study adds up to the few empirical studies that, to our knowledge, have associated purely Theta oscillatory activity with SN in humans (Caplan et al., 2001; Du et al., 2023; Gehrke & Gramann, 2021; Kahana et al., 1999).

What is more, we used an exploratory approach to inspect the data at single-trial level. This allowed us to capitalize on the complexity of the data at different levels of granularity. Dynamics of oscillatory episodes were rich, presenting patterns at different time-scales that can be related to the difficulty of the task (Theta band), access to encoded information (Theta band), and switch and focus of attention (Alpha band). On the one hand, we found that Theta correlates with global demands of the task, as increased Theta episode abundance was observed in the more difficult parts of the task at various time scales. At a longer time scale it increased from Immediate to Delayed recall; at a medium time-scale Theta abundance increased in the middle of the path compared to the beginning and end; and, at a short time scale within a single junction, frontal Theta abundance signalled the initial access to encoded information in anticipation of the impending navigational decision. On the other hand, Alpha oscillatory activity can be generally interpreted as a switch to internal attention, with increases in parietal episodes possibly signalling the inhibition of distracting sensory information to facilitate selective access to internal episodic representations.

In conclusion, the results of our study provide crucial support for long-standing theories linking Theta oscillatory activity with access to stored information relevant for SN. We addressed brain oscillations during task-relevant events at moment-to-moment single-trial level, and revealed a rich temporal, spatial, and spectral dynamics of brain activity during the resolution of SN tasks. Our methodological approach also provides proof of concept for future research aiming at singling out oscillatory activity from broadband activity in realistic SN dynamic tasks. In our opinion, such an analytical approach can help gain new insights into the role of oscillatory brain activity for SN in humans, as it provides access to the fine temporal structure of brain-behaviour correlations with non-invasive methods.

METHODS

Subjects

The experiment was run in accordance with the Declaration of Helsinki, under approval of the CEIC Parc de Salut Mar (Universitat Pompeu Fabra) institutional review board. All participants gave prior written informed consent, were naïve to the purpose of the experiment, and were compensated with 10 € per hour (in 30min fractions). Participant exclusion criteria were: history of epilepsy, being under medication for neurological or psychiatric disorders, and susceptibility of suffering motion sickness, screened online using the Cybersickness Susceptibility Questionnaire (Freiwald et al., 2020). 24 subjects were recruited for the experiment (13 female, 25±5 years), all were included in the final sample. The experimental session had an approximate duration of 3 hours.

Virtual Reality (VR) environment

The VR environment was programmed in Unity Real-Time Development Platform (Unity Technologies Inc., version 2020.3.19f1,) and was presented to subjects via a Head Mounted Display HTC Vive (HTC corporation) (Figure 9C). During navigation, subjects were seated and drove a car through streets using a steering wheel (Figure 9C). and one foot-pedal Logitech G29 (Logitech International S.A.)

The VR environment included three scenarios: resting area, habituation environment, and T-Junction mazes. Subjects entered the resting area (Figure 9B) on initiation of the experiment, where they could adjust their position, and align the virtual dashboard and the steering wheel with their own posture. In the resting area, a traffic light turned from red to green to indicate that subjects were allowed to proceed to the next scenario at a time of their choosing. Next, the habituation environment consisted of navigating a sequence of T-Junctions. Each arm of the maze consisted of a straight road ending with a T-crossing. Participants pressed the foot pedal to move forward, and were required to turn to left or right in time, before reaching a front wall, at the crossing. In this scenario subjects could freely choose to turn left or right. The purpose of the habituation environment was to familiarize subjects with the VR scenarios and the functioning of the steering wheel and pedal. After each turn, another T-junction started without a break in the visual flow, and subjects were allowed to drive in the habituation environment for as long as they required.

Finally, the T-Junction mazes environment used in the experiment, consisted of paths of 10 consecutive T-Junctions, similar to the habituation scenario. However, for each different maze there was a unique combination of left (L) and right (R) turns (for instance: LLRLRRRLRL) in order to reach the end point (target destination). If subjects took a wrong turn, they entered a dead end (Figure 9B) and were teleported to the resting area. Otherwise, they proceeded to the next arm of the maze until the end point, that was signalled by a tunnel. Once they successfully reached the end of a maze, subjects were teleported to the resting area. We created five different mazes for the experiment, plus an additional training maze (consist of 4 T-junctions). Each of the mazes simulated a succession of city-like streets with a unique, distinctive, combination of the following features: wall colour and texture, pavement texture, street elements (benches, lamps, plants), and window and door styles, all uninformative as to the correct path (Figures 9B-D).

Experimental protocol

The experiment took part in a laboratory room (CBC labs, Universitat Pompeu Fabra, Barcelona, Spain). On arrival, subjects were screened for susceptibility to cybersickness adverse symptoms (headache, blurred vision, eye strain) using the Simulator Sickness Questionnaire (Kennedy et al., 1993). None of the subjects reported severe symptoms and, therefore, all proceeded to the experiment. Next, subjects were seated on a chair, fitted with the VR goggles, and the SN paradigm started (Figure 9C). The paradigm was divided in two parts, separated by a distractor task. In Part I, the 5 mazes were learnt. For each maze, subjects first navigated the entire maze with direction cues indicating the correct turns (Guided mazes). Subjects had up to 3 attempts to correctly follow the path, but most participants completed the maze at the first attempt in this stage. Immediately after, they had 3 attempts to solve the same maze without directional cues (Immediate recall mazes). Each attempt ended either upon an

error or after successful completion. After studying the five different mazes, participants were allowed to exit the VR environment to take a resting break, during which they were invited to play the memory game Timeline (distractor task) for 15 minutes. After the break, Part II took place back in the VR environment. Subjects had to solve again the five mazes learnt in Part I, now presented in random order and without visual cues (Delayed recall mazes). EEG was recorded during both parts of the experiment, including 5 minutes recordings of resting activity (eyes closed) prior to the task.

Upon finishing, subjects filled out again the Simulator Sickness Questionnaire (Kennedy et al., 1993) to control for adverse symptoms due to the VR, and an immersion questionnaire adapted from Cárdenas-Delgado et al. (2017).

EEG acquisition and pre-processing

EEG was recorded during Part I and Part II of the experiment at a sampling rate of 500 Hz using a BrainAmp amplifier (BrainProducts, GmbH, Munich, Germany) with 61active electrodes (actiCAP, BrainProducts, GmbH, Munich, Germany) placed according to the 10-10 system. The ground electrode was placed at AFz and the online reference at the left mastoid. Two external electrodes were used for horizontal and vertical electrooculogram. Impedance was kept below 10 kΩ.

Pre-processing and segmentation were run using EEGLAB (Delorme & Makeig, 2004), Fieldtrip (Oostenveld et al., 2011) and custom-written code. First, noisy channels were detected using a combination of visual inspection and automatic procedures implemented with EEGLAB plugin *clean_rawdata* (flat channel for more than 10 seconds, high frequency noise above 4 standard deviations, correlation with neighbouring channels below 0.8). Noisy channels were discarded. Second, Independent Component Analysis (ICA) (Artoni et al., 2018) (extended *runica*) was used on continuous data to correct visual artefacts. *ICLabel* EEGLAB plugin (Pion-Tonachini et al., 2019) was used for the automatic labelling and discarding of components corresponding to blinks and eye movements, as well as muscle artefacts (cut-off threshold $p > 0.975$). Third, the data was re-referenced to the right mastoid and a high pass filter (Butterworth, order 4, non-causal, cut-off frequency 0.1 Hz) and a low pass filter (Butterworth, order 4, non-causal, cut-off frequency 80 Hz) were applied. Finally, pre-processed data was segmented in trials from -6500 to 500 ms relative to the turn onset, for the Immediate and Delayed recall mazes. The rejected channels were reconstructed using the data of neighbouring channels and spherical splines. Data recordings at rest (eyes closed) were pre-processed in the same way as SN task data and subsequently divided in epochs with the same duration of the task epochs. On average, 4±2 electrodes were marked as bad and interpolated across subjects. 2±1 visual components, and 3±2 muscle components were detected and discarded across subjects.

EEG analysis

EEG analysis was run using Fieldtrip (Oostenveld et al., 2011) and custom-written code. Data was down-sampled to 250 Hz. The frequencies of interest were Theta (3 to 8 Hz) and Alpha (8.5 to 14 Hz; range chosen to avoid spectral overlap with Theta band, the main frequency of interest). We used the *fBOSC* toolbox (Seymour et al., 2022) to identify oscillatory episodes.

Power was extracted in a time-resolved fashion within each epoch for frequencies in the 2 to 40 Hz range, 0.5 Hz steps, by means of Morlet wavelets (6 cycles). Oscillatory episodes were defined as segments of signal where power in the specified frequency exceeded the 99th percentile of background activity for at least 3 cycles. For each trial, electrode, and subject, we calculated the abundance (Seymour et al., 2022) of oscillatory episodes as the percentage of total time in which the signal presented oscillatory episodes in specified band (abundance is virtually equivalent to *p-episode*, in Caplan et al. 2001). We then detected the electrodes that presented higher Theta and Alpha abundance at group level during the SN. These electrodes were then selected for further single-subject and single-trial analyses.

Statistical analysis

We used linear mixed models (LMMs) for the statistical analysis, so that individual variability can be straightforwardly modelled using random factors. Because LMM can handle missing values and are robust to unbalanced designs they are convenient to consider simultaneously all the factors that can have an impact on the structure of the data (Verbeke & Molenberghs, 2009).

We divided the trials recorded during the SN task in segments of 2 second centred at times -5000 ms to -1000 ms before the turn (t=0) in steps of 2 seconds. Abundance, defined as the percentage of time in which an oscillatory episode was detected in the segment, was our variable of interest. Abundance is a continuous variable that can range from 0% (no oscillatory episode detected in the segment) to 100% (the whole segment consisted of oscillatory activity). Note that we excluded from the analysis the intervals -6500 to -6000 ms and 0 to 500 ms. Those intervals were excluded from because, on one side, we wanted to consider only data previous to turn and, on the other side, the abundance at the edges of the EEG segment can be underestimated.

We used a model with abundance as the dependent variable, participant as the random factor, and the fixed factors described in Table 1.

Statistical analysis was performed in R (R Core Team, 2022) with functions from the package *glmmTMB* (Brooks et al., 2017), using ordered beta family for the fit (see Supplementary Materials and Methods). In order to select the model that best described the data, we started from the full model:

$$Abundance \sim Stage + Run + Junction + \mathrm{Time} + Correct + Solved + (1|Participant),$$

and used the dredge function to build all possible models with this set of factors and *MuMIn* R package (Bartoń, K., 2009) to rank them according second order Akaike Information Criterion (AIC) (Burnham et al., 2010). Significance of the factors was assessed by means of ANOVA (type III X^2 test). Packages *superheat*(Barter & Yu, 2018) and *ggplot2*(Hadley Wickham, 2016) were used for visualization.

ACKNOWLEDGMENTS

This research was supported by grants from the *Ministerio de Ciencia e Innovación* (PID2022-137277NB-I00 AEI/FEDER) and PRESP05622 - PDC2022-133859-I00, and from AGAUR *Generalitat de Catalunya* (2021 SGR 00911) to S.S.F.

DATA AVAILABILITY

Pre-processed data and code required to replicate the analysis presented in this manuscript has been uploaded to a private project in Open Science Foundation. On acceptance of the manuscript, data and code will be made publicly available.

COMPETING INTERESTS

The authors declare no competing interests.

AUTHORS CONTRIBUTION

S.S.F. and M.T.C. conceptualized research, S.S.F., M.T.C., A.M.M. and M.S.P. designed research. A.M.M. and M.S.P. conducted research, M.T.C. analysed data. M.T.C., with the assistance of A.M.M., conducted statistical analysis. M.T.C. and S.S.F. wrote the manuscript. S.S.F. provided funding.

BIBLIOGRAPHY

Araújo, D. B. D., Baffa, O., & Wakai, R. T. (2002). Theta Oscillations and Human Navigation: A Magnetoencephalography Study. *Journal of Cognitive Neuroscience*, *14*(1), 70-78. https://doi.org/10.1162/089892902317205339

Arnau, Stefan, Brümmer, Tina, Liegel, Nathalie, & Wascher, Edmund. (2021). Inverse effects of time-on-task in task-related and task-unrelated theta activity. *Psychophysiology*, *58:e13805.* https://doi.org/10.1111/psyp.13805

Artoni, F., Delorme, A., & Makeig, S. (2018). Applying dimension reduction to EEG data by Principal Component Analysis reduces the quality of its subsequent Independent Component decomposition. *NeuroImage*, *175*, 176-187. https://doi.org/10.1016/j.neuroimage.2018.03.016

Barter, R. L., & Yu, B. (2018). Superheat: An R Package for Creating Beautiful and Extendable Heatmaps for Visualizing Complex Data. *Journal of Computational and Graphical Statistics*, *27*(4), 910-922. https://doi.org/10.1080/10618600.2018.1473780

Bartoń, K. (2009). *MuMIn: Multi-model inference (R package version 0.12.2)* [Software].

Bauer, M., Buckley, M. G., & Bast, T. (2021). Individual differences in theta-band oscillations in a spatial memory network revealed by electroencephalography predict rapid place learning. *Brain and Neuroscience Advances*, *5*, 239821282110027. https://doi.org/10.1177/23982128211002725

Baumann, O., & Mattingley, J. B. (2021). Extrahippocampal contributions to spatial navigation in humans: A review of the neuroimaging evidence. *Hippocampus*, *31*(7), 640-657. https://doi.org/10.1002/hipo.23313

Benedek, M., Schickel, R. J., Jauk, E., Fink, A., & Neubauer, A. C. (2014). Alpha power increases in right parietal cortex reflects focused internal attention. *Neuropsychologia*, *56*, 393-400. https://doi.org/10.1016/j.neuropsychologia.2014.02.010

Bischof, W. F., & Boulanger, P. (2003). Spatial Navigation in Virtual Reality Environments: An EEG Analysis. *Cyberpsychology and Behavior*, *6*(5), 487-495. https://doi.org/10.1089/109493103769710514

Bohbot, V. D., Copara, M. S., Gotman, J., & Ekstrom, A. D. (2017). Low-frequency theta oscillations in the human hippocampus during real-world and virtual navigation. *Nature Communications*, *8*, 1-7. https://doi.org/10.1038/ncomms14415

Bonnefond, M., & Jensen, O. (2012). Alpha Oscillations Serve to Protect Working Memory Maintenance against Anticipated Distracters. *Current Biology*, *22*(20), 1969-1974. https://doi.org/10.1016/j.cub.2012.08.029

Brooks, M., E., Kristensen, K., Benthem, K., J. ,van, Magnusson, A., Berg, C., W., Nielsen, A., Skaug, H., J., Mächler, M., & Bolker, B., M. (2017). glmmTMB Balances Speed and Flexibility Among Packages for Zero-inflated Generalized Linear Mixed Modeling. *The R Journal*, *9*(2), 378. https://doi.org/10.32614/RJ-2017-066

Burnham, K. P., Anderson, D. R., & Anderson, D. R. (2010). *Model selection and multimodel inference: A practical information-theoretic approach* (2. ed., [4. printing]). Springer.

Burns, P. C. (1999). Navigation and the mobility of older drivers. *Journals of Gerontology - Series B Psychological Sciences and Social Sciences*, *54*(1), 49-55. https://doi.org/10.1093/geronb/54B.1.S49

Buzsáki, G. (2005). Theta rhythm of navigation: Link between path integration and landmark navigation, episodic and semantic memory. *Hippocampus*, *15*(7), 827-840. https://doi.org/10.1002/hipo.20113

Buzsáki, G., & Moser, E. I. (2013). Memory, navigation and theta rhythm in the hippocampal-entorhinal system. *Nature Neuroscience*, *16*(2), 130-138. https://doi.org/10.1038/nn.3304

Caplan, J. B., Madsen, J. R., Raghavachari, S., & Kahana, M. J. (2001). Distinct patterns of brain oscillations underlie two basic parameters of human maze learning. *Journal of neurophysiology*, *86*(1), 368-380. https://doi.org/10.1152/jn.2001.86.1.368

Cárdenas-Delgado, S., Méndez-López, M., Juan, M.-C., Pérez-Hernández, E., Lluch, J., & Vivó, R. (2017). Using a Virtual Maze Task to Assess Spatial Short-term Memory in Adults: *Proceedings of the 12th International Joint Conference on Computer Vision, Imaging and Computer Graphics Theory and Applications*, 46-57. https://doi.org/10.5220/0006093200460057

Cavanagh, J. F., & Frank, M. J. (2014). Frontal theta as a mechanism for cognitive control. *Trends in Cognitive Sciences*, *18*(8), 414-421. https://doi.org/10.1016/j.tics.2014.04.012

Chrastil, E. R., Rice, C., Goncalves, M., Moore, K. N., Wynn, S. C., Stern, C. E., & Nyhus, E. (2022). Theta oscillations support active exploration in human spatial navigation. *NeuroImage*, *262*, 119581. https://doi.org/10.1016/j.neuroimage.2022.119581

Cogné, M., Taillade, M., N'Kaoua, B., Tarruella, A., Klinger, E., Larrue, F., Sauzéon, H., Joseph, P. A., & Sorita, E. (2017). The contribution of virtual reality to the diagnosis of spatial navigation disorders and to the study of the role of navigational aids: A systematic literature review. *Annals of Physical and Rehabilitation Medicine*, *60*(3), 164-176. https://doi.org/10.1016/j.rehab.2015.12.004

Cushman, L. A., Stein, K., & Duffy, C. J. (2008). Detecting navigational deficits in cognitive aging and Alzheimer disease using virtual reality. *Neurology*, *71*(12), 888-895. https://doi.org/10.1212/01.wnl.0000326262.67613.fe

Delorme, A., & Makeig, S. (2004). EEGLAB: An open source toolbox for analysis of single-trial EEG dynamics including independent component analysis. *Journal of Neuroscience Methods*, *134*(1), 9-21. https://doi.org/10.1016/j.jneumeth.2003.10.009

Diersch, N., & Wolbers, T. (2019). The potential of virtual reality for spatial navigation research across the adult lifespan. *Journal of Experimental Biology*, *222*. https://doi.org/10.1242/jeb.187252

Do, T.-T. N., Lin, C.-T., & Gramann, K. (2021). Human brain dynamics in active spatial navigation. *Scientific Reports*, *11*(1), 13036. https://doi.org/10.1038/s41598-021-92246-4

Do, T.-T. N., Singh, A. K., Cortes, C. A. T., & Lin, C.-T. (2020). Estimating the cognitive load in physical spatial navigation. *2020 IEEE Symposium Series on Computational Intelligence (SSCI)*, 568-575. https://doi.org/10.1109/SSCI47803.2020.9308389

Donoghue, T., Schaworonkow, N., & Voytek, B. (2022). Methodological considerations for studying neural oscillations. *European Journal of Neuroscience*, *55*(11-12), 3502-3527. https://doi.org/10.1111/ejn.15361

Du, Y. K., Liang, M., McAvan, A. S., Wilson, R. C., & Ekstrom, A. D. (2023). Frontal-midline theta and posterior alpha oscillations index early processing of spatial representations during active navigation. *Cortex*, *169*, 65-80. https://doi.org/10.1016/j.cortex.2023.09.005

Eichenbaum, H. (2017). The role of the hippocampus in navigation is memory. *Journal of Neurophysiology*, *117*(4), 1785-1796. https://doi.org/10.1152/jn.00005.2017

Ekstrom, A. D., Caplan, J. B., Ho, E., Shattuck, K., Fried, I., & Kahana, M. J. (2005). *Human Hippocampal Theta Activity During Virtual Navigation*. *889*, 881-889. https://doi.org/10.1002/hipo.20109

Ekstrom, A. D., Huffman, D. J., & Starrett, M. (2017). Interacting networks of brain regions underlie human spatial navigation: A review and novel synthesis of the literature. *Journal of Neurophysiology*, *118*(6), 3328-3344. https://doi.org/10.1152/jn.00531.2017

Epstein, R. A., Patai, E. Z., Julian, J. B., & Spiers, H. J. (2017). The cognitive map in humans: Spatial navigation and beyond. *Nature Neuroscience*, *20*(11), 1504-1513. https://doi.org/10.1038/nn.4656

Freiwald, J. P., Göbel, Y., Mostajeran, F., & Steinicke, F. (2020). The cybersickness susceptibility questionnaire: Predicting virtual reality tolerance. *Proceedings of Mensch Und Computer 2020*, 115-118. https://doi.org/10.1145/3404983.3410022

Gehrke, L., & Gramann, K. (2021). Single-trial regression of spatial exploration behavior indicates posterior EEG alpha modulation to reflect egocentric coding. *European Journal of Neuroscience*, *54*(12), 8318-8335. https://doi.org/10.1111/ejn.15152

Gerster, M., Waterstraat, G., Litvak, V., Lehnertz, K., Schnitzler, A., Florin, E., Curio, G., & Nikulin, V. (2022). Separating Neural Oscillations from Aperiodic 1/f Activity: Challenges and Recommendations. *Neuroinformatics*, *20*(4), 991-1012. https://doi.org/10.1007/s12021-022-09581-8

Gilden, D. L. (2001). Cognitive Emissions of 1/f Noise. *Psychological Review*, *108*(1), 33-56. https://doi.org/10.I037//0033-295X.108.1.33

Hadley Wickham. (2016). *ggplot2: Elegant Graphics for Data Analysis*. Springer-Verlag. https://ggplot2.tidyverse.org

Hilton, C., Kapaj, A., & Fabrikant, S. I. (2023). Landmark Sequence Learning from Real-World Route Navigation and the Impact of Navigation Aid Visualisation Style. *Journal of Cognition*, *6*(1), 41. https://doi.org/10.5334/joc.307

Hyman, J. M., Zilli, E. A., Paley, A. M., & Hasselmo, M. E. (2005). Medial prefrontal cortex cells show dynamic modulation with the hippocampal theta rhythm dependent on behavior. *Hippocampus*, *15*(6), 739-749. https://doi.org/10.1002/hipo.20106

Jacobs, J., Korolev, I. O., Caplan, J. B., Ekstrom, A. D., Litt, B., Baltuch, G., Fried, I., Schulze-Bonhage, A., Madsen, J. R., & Kahana, M. J. (2010). Right-lateralized Brain Oscillations

in Human Spatial Navigation. *Journal of Cognitive Neuroscience*, *22*(5), 824-836. https://doi.org/10.1162/jocn.2009.21240

Jensen, O. (2024). Distractor inhibition by alpha oscillations is controlled by an indirect mechanism governed by goal-relevant information. *Communications Psychology*, *2*(1), 1-11. https://doi.org/10.1038/s44271-024-00081-w

Jones, S. R. (2016). When brain rhythms aren't 'rhythmic': Implication for their mechanisms and meaning. *Current Opinion in Neurobiology*, *40*, 72-80. https://doi.org/10.1016/j.conb.2016.06.010

Kahana, M. J., Sekuler, R., Caplan, J. B., Kirschen, M., & Madsen, J. R. (1999). Human theta oscillations exhibit task dependence during virtual maze navigation. *Nature*, *399*(6738), 781-784. https://doi.org/10.1038/21645

Kennedy, R. S., Lane, N. E., Berbaum, K. S., & Lilienthal, M. G. (1993). Simulator Sickness Questionnaire: An Enhanced Method for Quantifying Simulator Sickness. *The International Journal of Aviation Psychology*, *3*(3), 203-220. https://doi.org/10.1207/s15327108ijap0303_3

Klimesch, W. (2012). Alpha-band oscillations, attention, and controlled access to stored information. *Trends in Cognitive Sciences*, *16*(12), 606-617. https://doi.org/10.1016/j.tics.2012.10.007

Liang, M., Starrett, M. J., & Ekstrom, A. D. (2018). Dissociation of frontal-midline delta-theta and posterior alpha oscillations: A mobile EEG study. *Psychophysiology*, *55*(9), 1-14. https://doi.org/10.1111/psyp.13090

Magosso, E., De Crescenzio, F., Ricci, G., Piastra, S., & Ursino, M. (2019). EEG Alpha Power Is Modulated by Attentional Changes during Cognitive Tasks and Virtual Reality Immersion. *Computational Intelligence and Neuroscience*, *2019*, 1-18. https://doi.org/10.1155/2019/7051079

Magosso, E., Ricci, G., & Ursino, M. (2021). Alpha and theta mechanisms operating in internal-external attention competition. *Journal of Integrative Neuroscience*, *20*(1), 1. https://doi.org/10.31083/j.jin.2021.01.422

O'Keefe, J., & Conway, D. H. (1978). Hippocampal place units in the freely moving rat: Why they fire where they fire. *Experimental Brain Research*, *31*(4), 573-590. https://doi.org/10.1007/BF00239813

O'Keefe, J., & Nadel, L. (1978). *The hippocampus as a cognitive map*. Clarendon Press; Oxford University Press.

Oostenveld, R., Fries, P., Maris, E., & Schoffelen, J.-M. (2011). FieldTrip: Open Source Software for Advanced Analysis of MEG, EEG, and Invasive Electrophysiological Data. *Computational Intelligence and Neuroscience*, *2011*, 1-9. https://doi.org/10.1155/2011/156869

Ouyang, G., Hildebrandt, A., Schmitz, F., & Herrmann, C. S. (2020). Decomposing alpha and 1/f brain activities reveals their differential associations with cognitive processing speed. *NeuroImage*, *205*, 116304. https://doi.org/10.1016/j.neuroimage.2019.116304

Patai, E. Z., & Spiers, H. J. (2021). The Versatile Wayfinder: Prefrontal Contributions to Spatial Navigation. *Trends in Cognitive Sciences*, *25*(6), 520-533. https://doi.org/10.1016/j.tics.2021.02.010

Pion-Tonachini, L., Kreutz-Delgado, K., & Makeig, S. (2019). ICLabel: An automated electroencephalographic independent component classifier, dataset, and website. *NeuroImage*, *198*, 181-197. https://doi.org/10.1016/j.neuroimage.2019.05.026

Plácido, J., de Almeida, C. A. B., Ferreira, J. V., de Oliveira Silva, F., Monteiro-Junior, R. S., Tangen, G. G., Laks, J., & Deslandes, A. C. (2022). Spatial navigation in older adults with mild cognitive impairment and dementia: A systematic review and meta-analysis. *Experimental Gerontology*, *165*(April). https://doi.org/10.1016/j.exger.2022.111852

Podvalny, E., Noy, N., Harel, M., Bickel, S., Chechik, G., Schroeder, C. E., Mehta, A. D., Tsodyks, M., & Malach, R. (2015). A unifying principle underlying the extracellular field potential spectral responses in the human cortex. *J Neurophysiol*, *114*. https://doi.org/doi:10.1152/jn.00943.2014

R Core Team. (2022). *R: A Language and Environment for Statistical Computing. R Foundation for Statistical Computing* [Software]. R Foundation for Statistical Computing. https://www.R-project.org/

Samaha, J., & Cohen, M. X. (2022). Power spectrum slope confounds estimation of instantaneous oscillatory frequency. *NeuroImage*, *250*, 118929. https://doi.org/10.1016/j.neuroimage.2022.118929

Schmidt, R., Diba, K., Leibold, C., Schmitz, D., Buzsáki, G., & Kempter, R. (2009). Single-Trial Phase Precession in the Hippocampus. *The Journal of Neuroscience*, *29*(42), 13232-13241. https://doi.org/10.1523/JNEUROSCI.2270-09.2009

Seymour, R. A., Alexander, N., & Maguire, E. A. (2022). Robust estimation of 1/f activity improves oscillatory burst detection. *European Journal of Neuroscience*, *56*(10), 5836-5852. https://doi.org/10.1111/ejn.15829

Thornberry, C., Caffrey, M., & Commins, S. (2023). Theta oscillatory power decreases in humans are associated with spatial learning in a virtual water maze task. *European Journal of Neuroscience*, *58*(11), 4341-4356. https://doi.org/10.1111/ejn.16185

Tolman, E. C. (1948). Cognitive Map in Rats and Men. *Psychological Review*, *55*(4), 189-208. https://doi.org/10.1037/h0061626

Tran, Y., Craig, A., Craig, R., Chai, R., & Nguyen, H. (2020). The influence of mental fatigue on brain activity: Evidence from a systematic review with meta-analyses. *Psychophysiology*, *57:e13554*. https://doi.org/10.1111/psyp.13554

Verbeke, G., & Molenberghs, G. M. (2009). *Linear Mixed Models for Longitudinal Data*. Springer US. https://doi.org/10.1007/978-1-4419-0300-6

Waschke, L., Donoghue, T., Fiedler, L., Smith, S., Garrett, D. D., Voytek, B., & Obleser, J. (2021). Modality--specific tracking of attention and sensory statistics in the human electrophysiological spectral exponent. *eLife*, *0:e70068*. https://doi.org/DOI: https://doi.org/10.7554/eLife.70068

White, D. J., Congedo, M., Ciorciari, J., & Silberstein, R. B. (2012). Brain Oscillatory Activity during Spatial Navigation: Theta and Gamma Activity Link Medial Temporal and Parietal Regions. *Journal of Cognitive Neuroscience*, *24*(3), 686-697. https://doi.org/10.1162/jocn_a_00098

Zhu, B., Cruz-Garza, J. G., Yang, Q., Shoaran, M., & Kalantari, S. (2022). Identifying uncertainty states during wayfinding in indoor environments: An EEG classification study. *Advanced Engineering Informatics*, *54*, 101718. https://doi.org/10.1016/j.aei.2022.101718

FIGURE CAPTIONS

Figure 1: Average number of correct junctions recalled in the Immediate recall mazes (left) and Delayed recall mazes (right). Grey dots correspond to individual data and black dots correspond to the average across subjects, error bars correspond to the standard error of the mean.

Figure 2: **A:** Distribution of episodes across frequency and electrodes. **B:** Topographical distribution of Theta (3 to 8 Hz) episodes. **C:** Topographical distribution of Alpha (8.5 to 14 Hz) episodes. **D:** Episode abundance for channels Fz (black) and Pz (red) during the SN task. **E:** Episode abundance for channels Fz (black) and Pz (red) at rest. **F:** Example of the EEG trace during the SN for a subject (black) with two oscillatory episodes identified (red). Time 0 corresponds to onset of the decision.

Figure 3: Individual abundance values averaged across time, electrodes and trials for Theta and Alpha bands. Each point corresponds to one subject. Distribution of oscillatory episodes is shown in the top (Theta) and Right (Alpha) histograms.

Figure 4: Mean episode abundance for Immediate recall (grey) and Delayed recall (black) mazes. Values are z-scored with respect to values shown in Figure 3. Theta band **A** and **F:** Abundance as a function of Run. **B** and **G:** Abundance as a function of Junction within a maze. **C** and **H:** Abundance as a function of Time within the approach to a junction turn, averaged in 2 s bins centred at -1, -3 and -.5 s prior to the turn **D** and **I:** Abundance as a function of decision accuracy in the upcoming turn. **E** and **J:** Abundance averaged across the whole maze, as a function of whether the maze was solved correctly or not. Error bars indicate the 95% CI.

Figure 5: The central plot displays the time-resolved mean Theta episode abundance values as a function of Junction within a maze (y axis) and Time to decision within a Junction approach (x-axis). For each subject, Abundance was z-scored with respect to the individual Theta episode abundance values displayed in Figure 3. The top plot displays abundance as a function of Time

to decision within a junction approach averaged across all junctions, and the right margin plot displays abundance as a function of Junction, averaged across Time within the Junction approach. Lines correspond to locally estimated scatterplot smoothing and shaded areas to the standard error of the estimation.

Figure 6: The central plot displays the time-resolved mean Alpha episode abundance values as a function of Junction within a maze (y axis) and Time to decision within a Junction approach (x-axis). For each subject, Abundance was z-scored with respect to the individual Alpha episode abundance values displayed in Figure 3. The top plot displays abundance as a function of Time to decision within a junction approach averaged across all junctions, and the right margin plot displays abundance as a function of Junction, averaged across Time within the Junction approach. Lines correspond to locally estimated scatterplot smoothing and shaded areas to the standard error of the estimation.

Figure 7: Predicted abundance values for Theta (**A** to **D**) and Alpha (**E** to **H**) frequency bands. **A** and **E**: Immediate (IR) and Delayed (DR) recall trials. **B** and **F**: As a function of junction. **C** and **G**: As a function of time to decision. **D**: As a function of run. **H**: For correct and incorrect decisions.

Figure 8: Summary of episode abundance across different time-scales. At a long time-scale, both Frontal Theta and Parietal Alpha episode abundance increased in Delayed Recall trials compared to Immediate recall trials. Within a maze time-scale (approximately 2 minutes), frontal Theta episodes abundance significantly increased in the middle part of the maze (in particular, at junctions 5 and 6) compared to the start and end of the maze, whereas Parietal Alpha increased in junctions 3 and 4 compared to first junction. In a junction, episode abundance for both Frontal Theta and Parietal alpha was maximal at the start of the junction and progressively decreased when subjects approached the decision point. Last, Alpha episodes abundance was significantly higher for trials preceding a correct decision compared to an erroneous one.

Figure 9: **A:** Experimental procedure: Subjects entered first a habituation environment consisting in T-junctions, they were instructed on using the steering wheel and pedal. They were allowed to stay in the environment until they were familiar with the commands. Next, participants performed a training, consisting on a short version of the mazes presented in Part I. In Part 1, 5 T-Junction mazes (10 junctions each) were presented in randomized order. Each of the maze was presented consecutively in 2 modalities: Guided and Immediate recall. For each modality, subjects had up to 3 attempts to solve the maze. After completion of Part I, subjects took a break, removed the HMD and performed a distractor task: they played a Timeline card game (Zygomatic) against the experimenter. Finally, subjects entered the VR again and performed the Delayed recall: they were presented with the mazes learnt in Part I, in randomized order. Each maze was presented without visual cues and subjects had up to 5 attempts to solve it. During all the virtual navigation, white noise was provided to subjects by means of earbuds. B: Snapshots of the VR environment: Resting area that subjects entered after an error or after successfully solving a maze. Subjects were allowed to rest there as long as they required before entering the next maze. In the Guided modality, visual cues (traffic signs with arrows) indicated which was the correct side to turn. In the Immediate and Delayed recall modality, the mazes were the same as the ones presented in the Guided modality, but visual cues were removed. When subjects committed an error, they entered a dead end and were teleported to the resting area. **C**: Image of a subject performing the task.

TABLES

Factor	Range	Description
Stage	1 or 2	1: Immediate recall trials, 2: Delayed recall trials
Run	1,2,3 (Immediate recall) or 1,2…5 (Delayed	Attempt number to solve a given maze in a given stage. Scales with familiarity.

	recall)	
Junction	1, 2…10	Turn number the subject is about to take in a given maze. Corresponds to the location within a path.
Correct	0 or 1	If true (1), subject recalled correctly the direction to turn in the upcoming junction
Solved	0 or 1	If true (1), the epoch considered is part of a run in which the subject provided 10 consecutive correct decisions. Scales with familiarity.
Time	-5, -3, -1	Time before the junction and decision of the turn direction. Is related to distance to the upcoming turn.

Table 1: Factors included in the LMM.

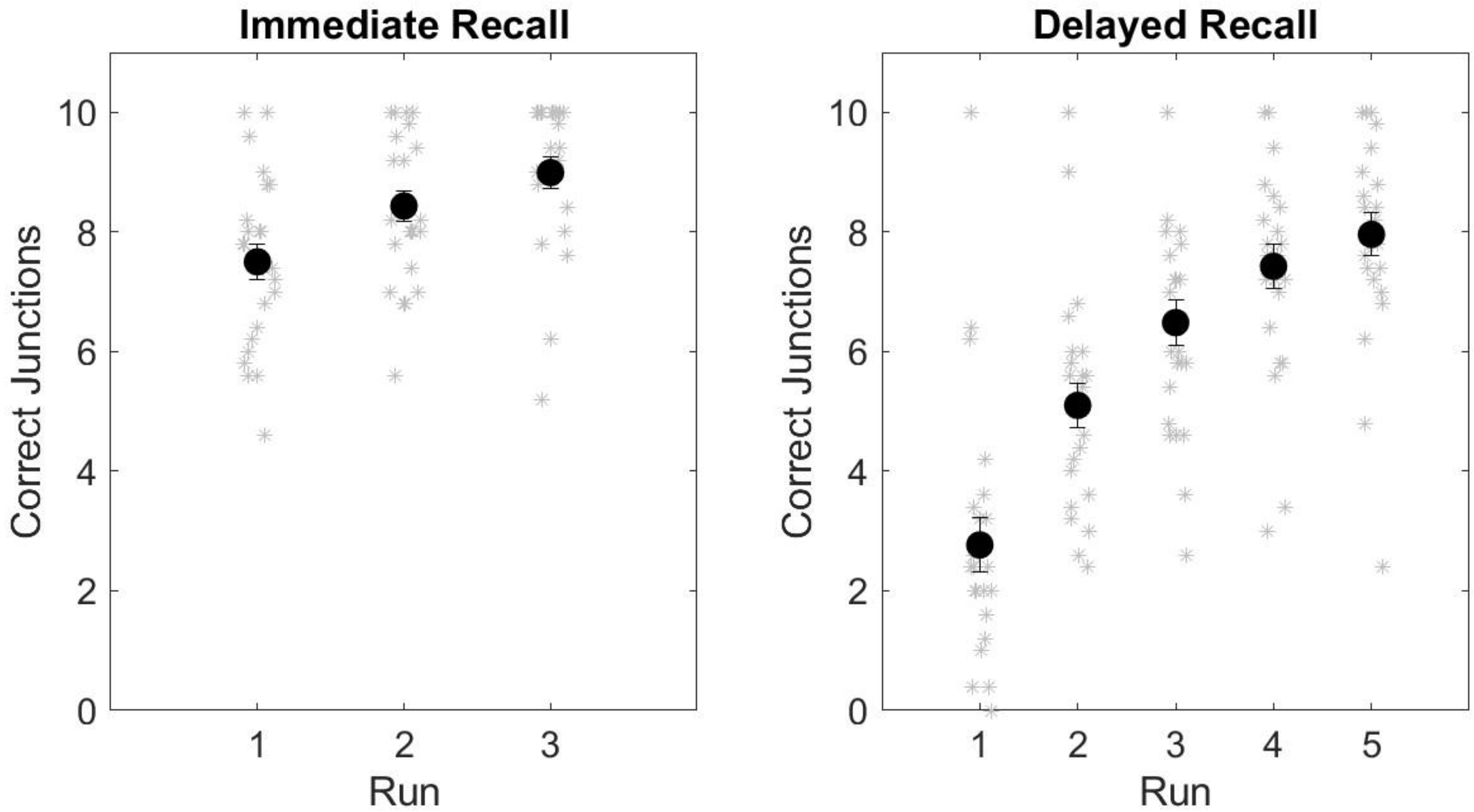
Immediate Recall
Delayed Recall
Correct Junctions
Run
0
2
4
6
8
10
1
2
3
4
5

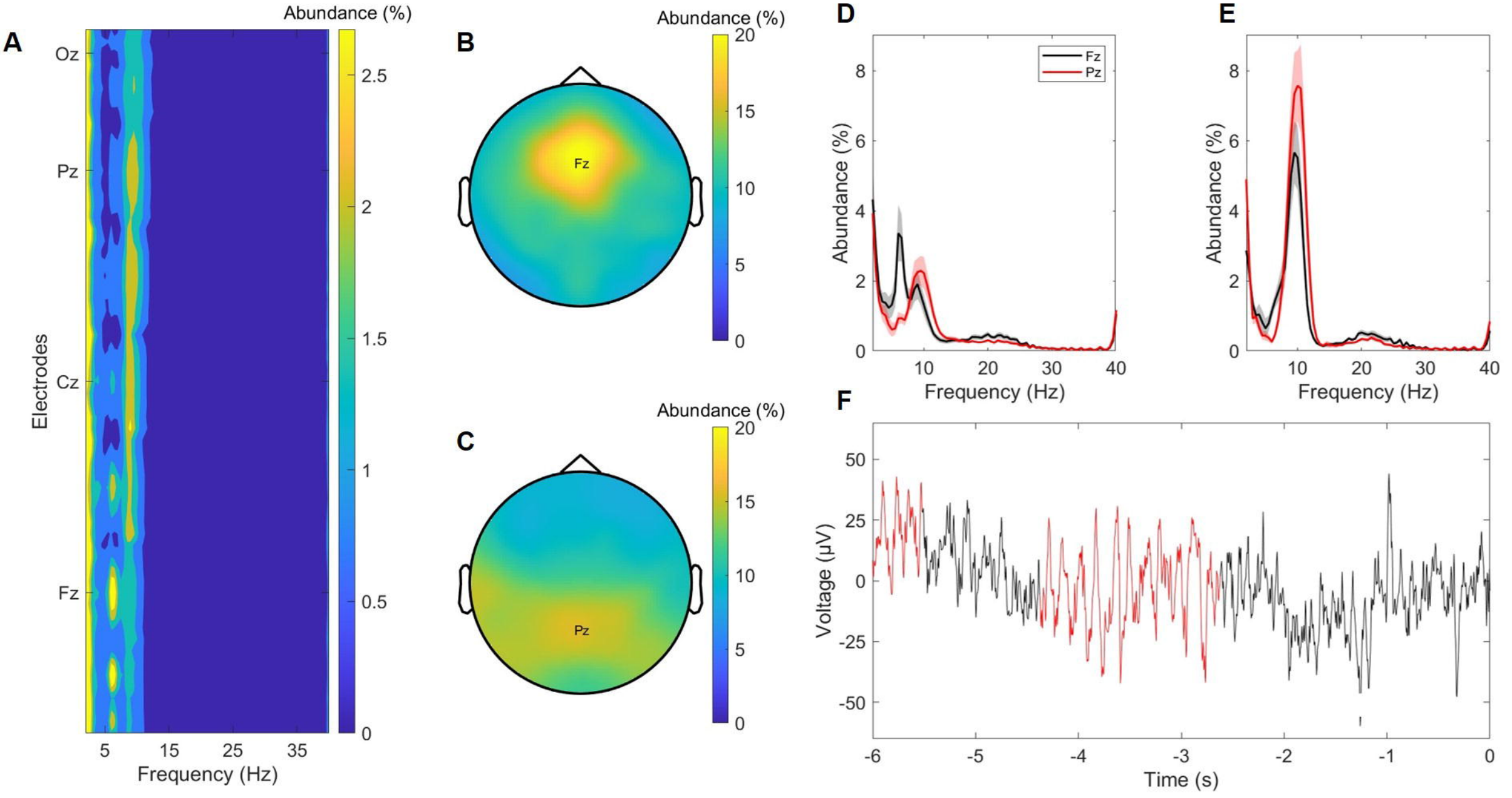
A
Abundance (%)
Oz
Pz
Cz
Fz
Electrodes
5
15
25
35
Frequency (Hz)
2.5
2
1.5
1
0.5
0
B
Abundance (%)
Fz
20
15
10
5
0
C
Abundance (%)
Pz
20
15
10
5
0
D
Fz
Pz
Abundance (%)
Frequency (Hz)
E
Abundance (%)
Frequency (Hz)
F
Voltage (µV)
Time (s)

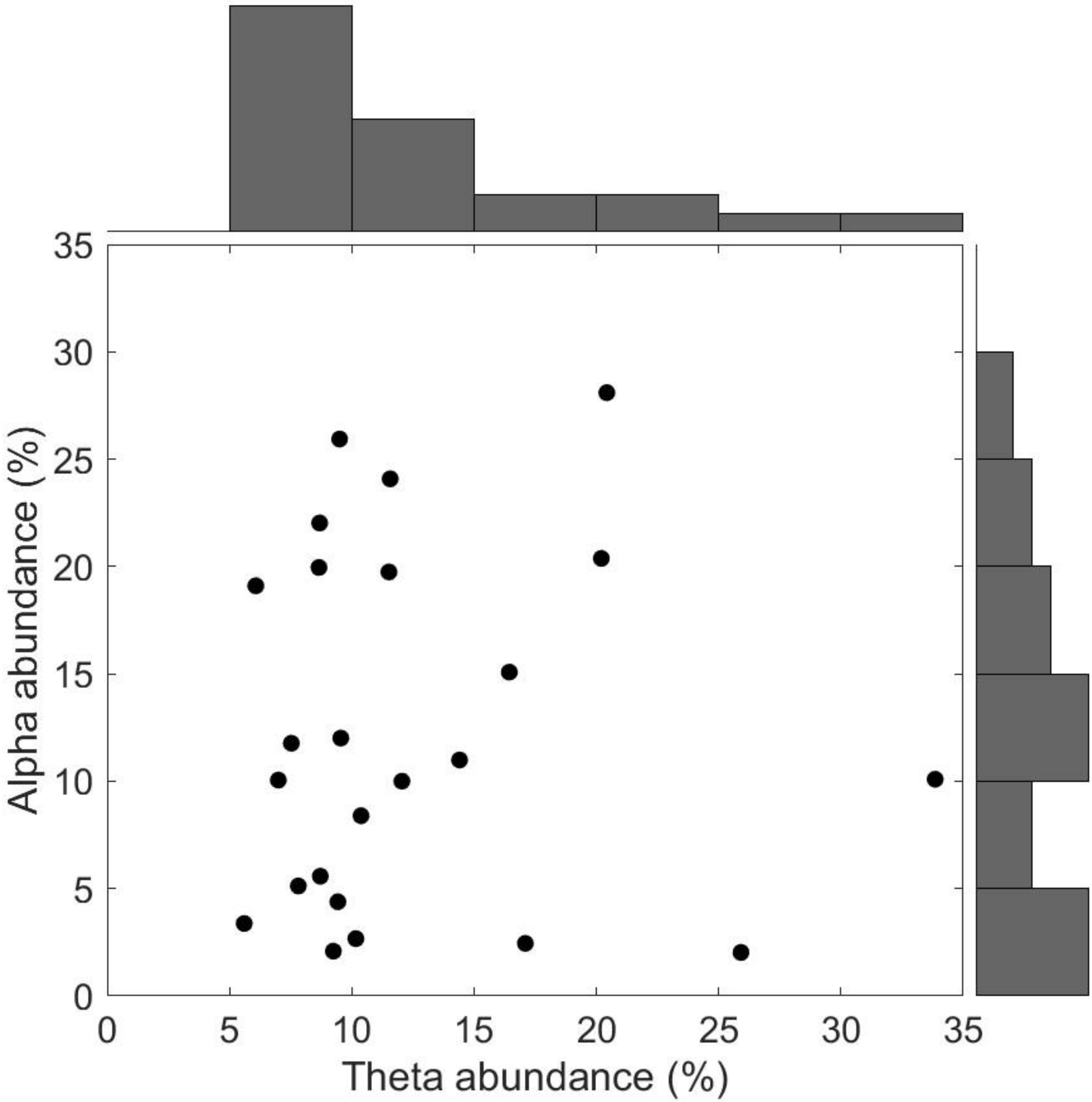
35
30
25
20
15
10
5
0
Alpha abundance (%)
0
5
10
15
20
25
30
35
Theta abundance (%)

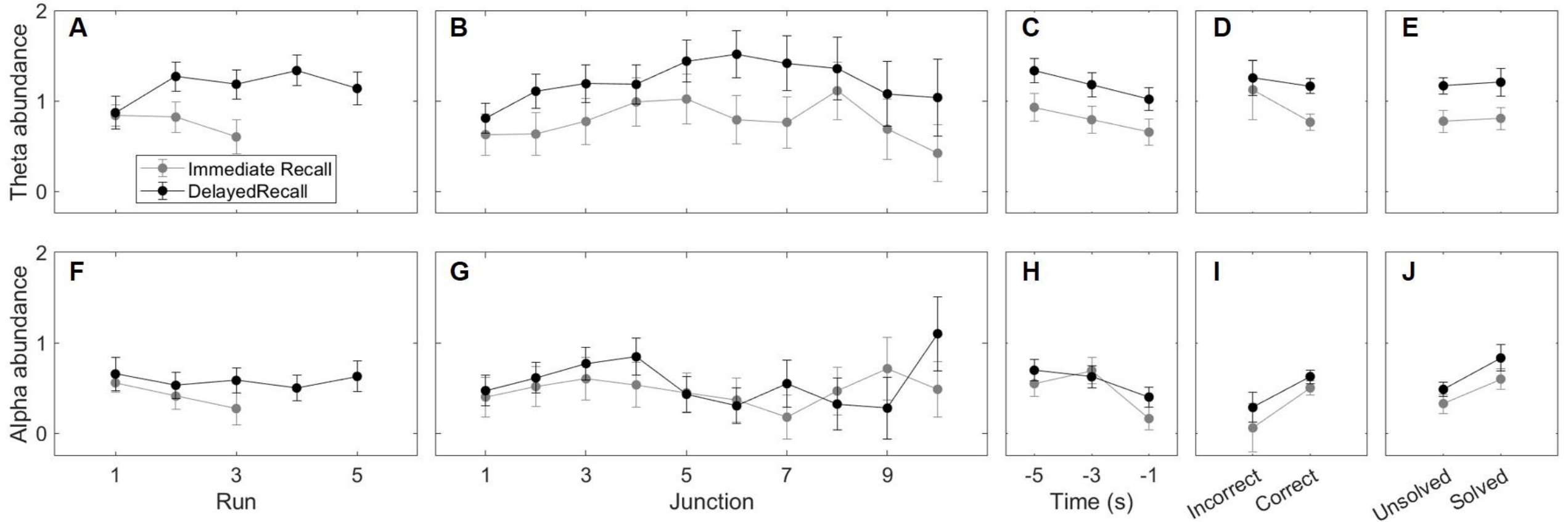
A
B
C
D
E
F
G
H
I
J
Theta abundance
Alpha abundance
2
1
0
Immediate Recall
DelayedRecall
1
3
5
Run
1
3
5
7
9
Junction
-5
-3
-1
Time (s)
Incorrect
Correct
Unsolved
Solved

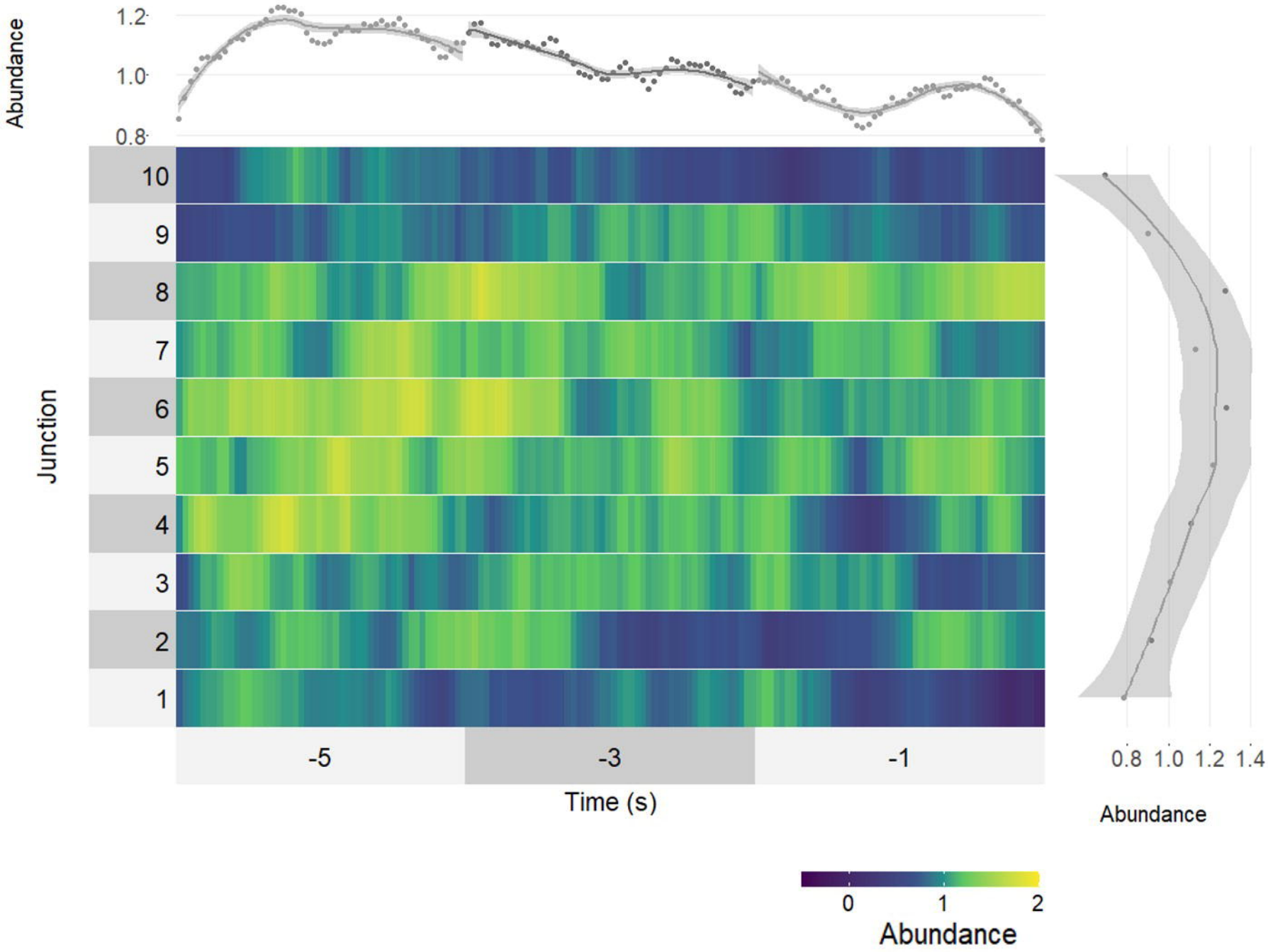
Abundance
1.2
1.0
0.8
Junction
10
9
8
7
6
5
4
3
2
1
-5
-3
-1
Time (s)
0.8
1.0
1.2
1.4
Abundance
0
1
2
Abundance

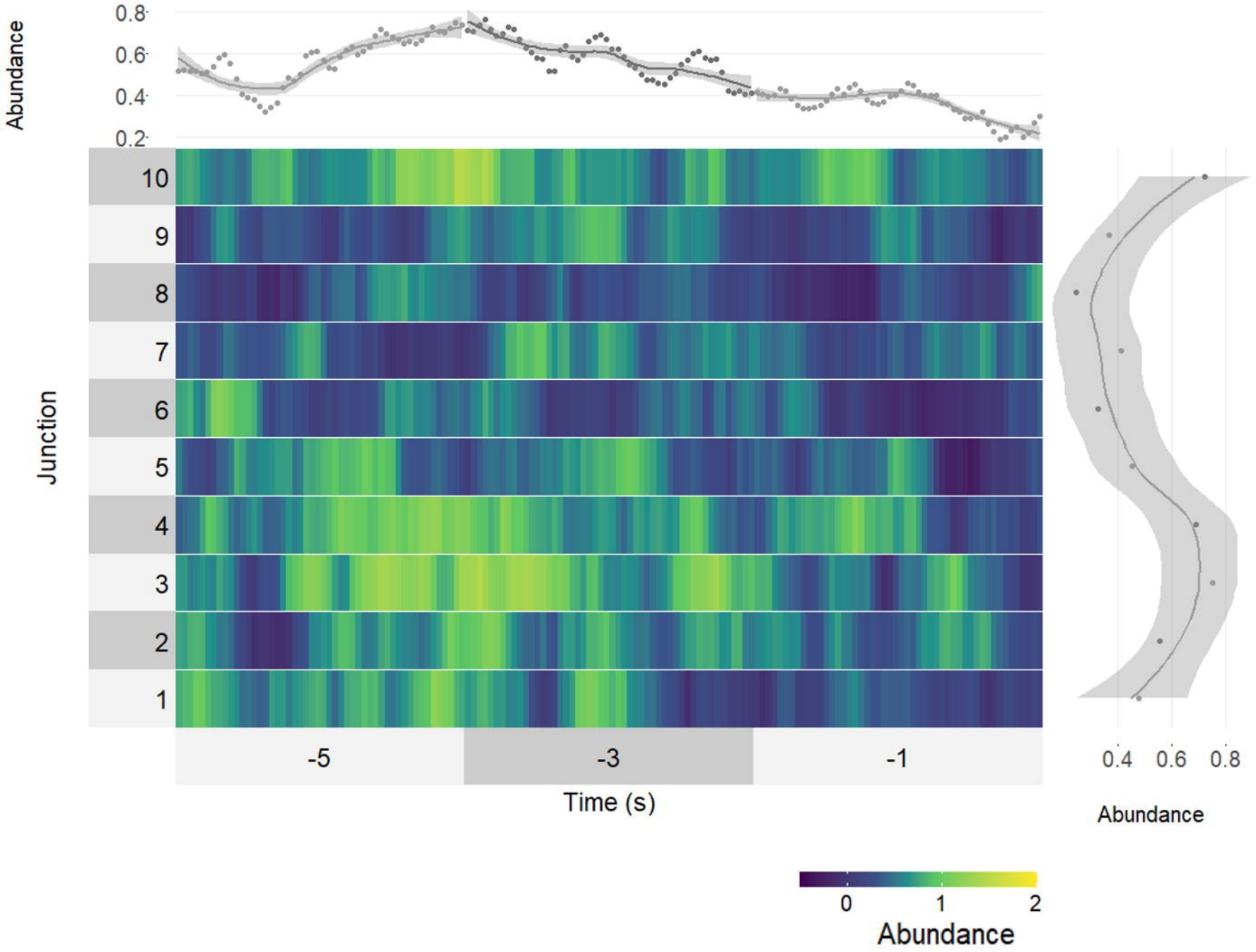
Abundance
0.8
0.6
0.4
0.2
Junction
10
9
8
7
6
5
4
3
2
1
-5
-3
-1
Time (s)
0.4
0.6
0.8
Abundance
0
1
2
Abundance

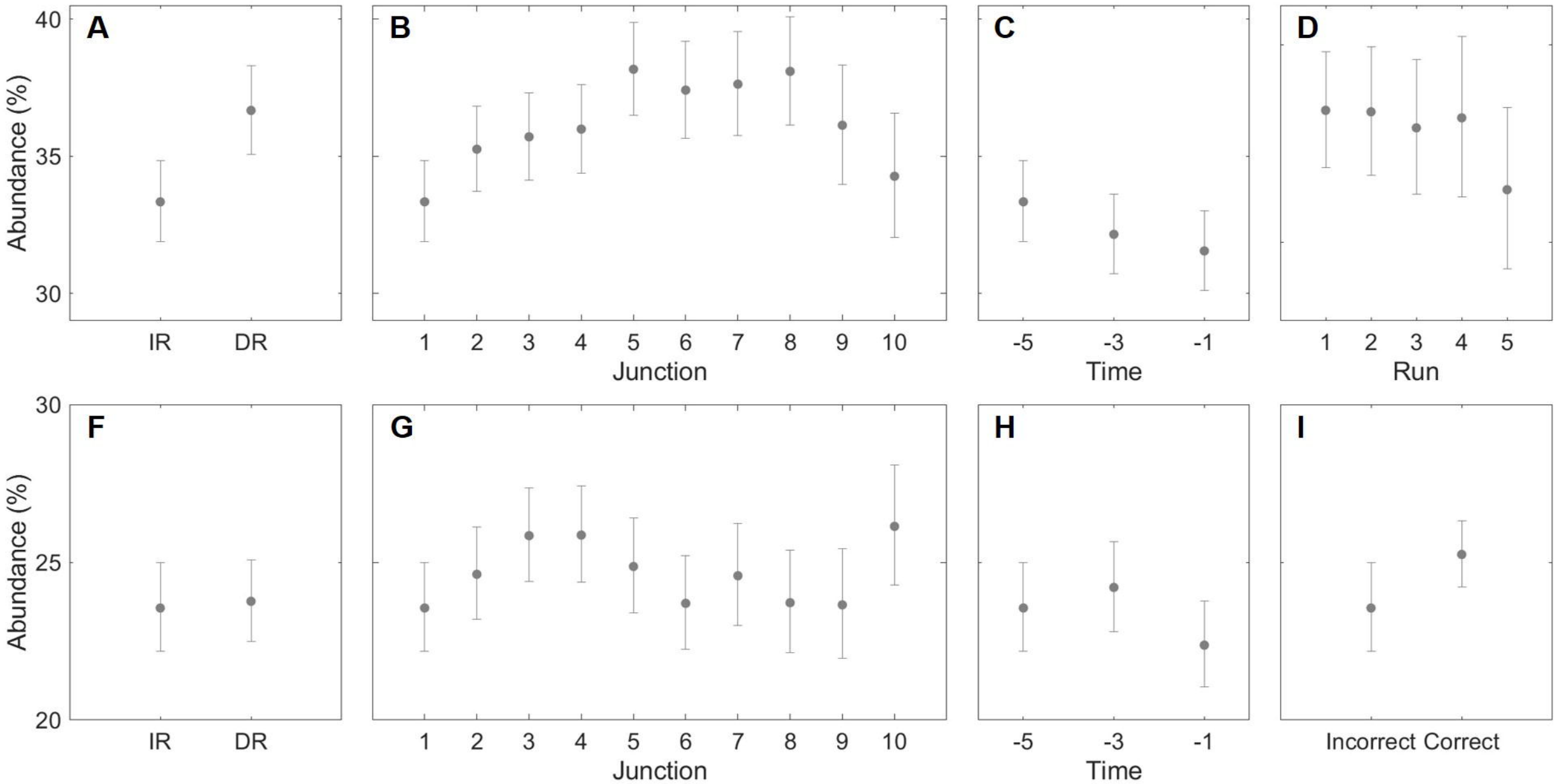
A
B
C
D
F
G
H
I
Abundance (%)
40
35
30
25
20
IR
DR
1
2
3
4
5
6
7
8
9
10
Junction
-5
-3
-1
Time
Run
Incorrect
Correct

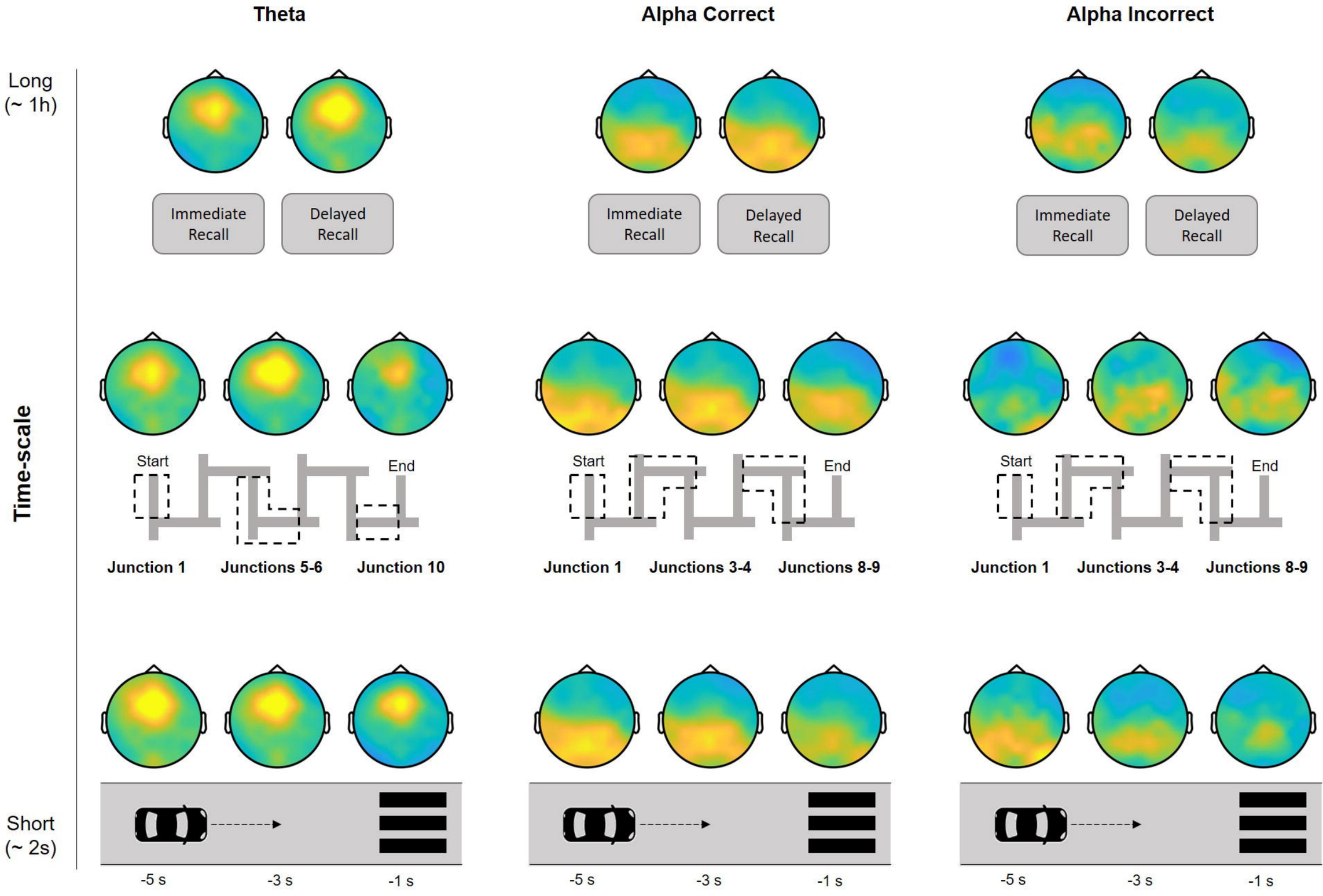
Theta
Alpha Correct
Alpha Incorrect
Long
(~ 1h)
Immediate Recall
Delayed Recall
Immediate Recall
Delayed Recall
Immediate Recall
Delayed Recall
Time-scale
Start
End
Junction 1
Junctions 5-6
Junction 10
Start
End
Junction 1
Junctions 3-4
Junctions 8-9
Start
End
Junction 1
Junctions 3-4
Junctions 8-9
Short
(~ 2s)
-5 s
-3 s
-1 s
-5 s
-3 s
-1 s
-5 s
-3 s
-1 s

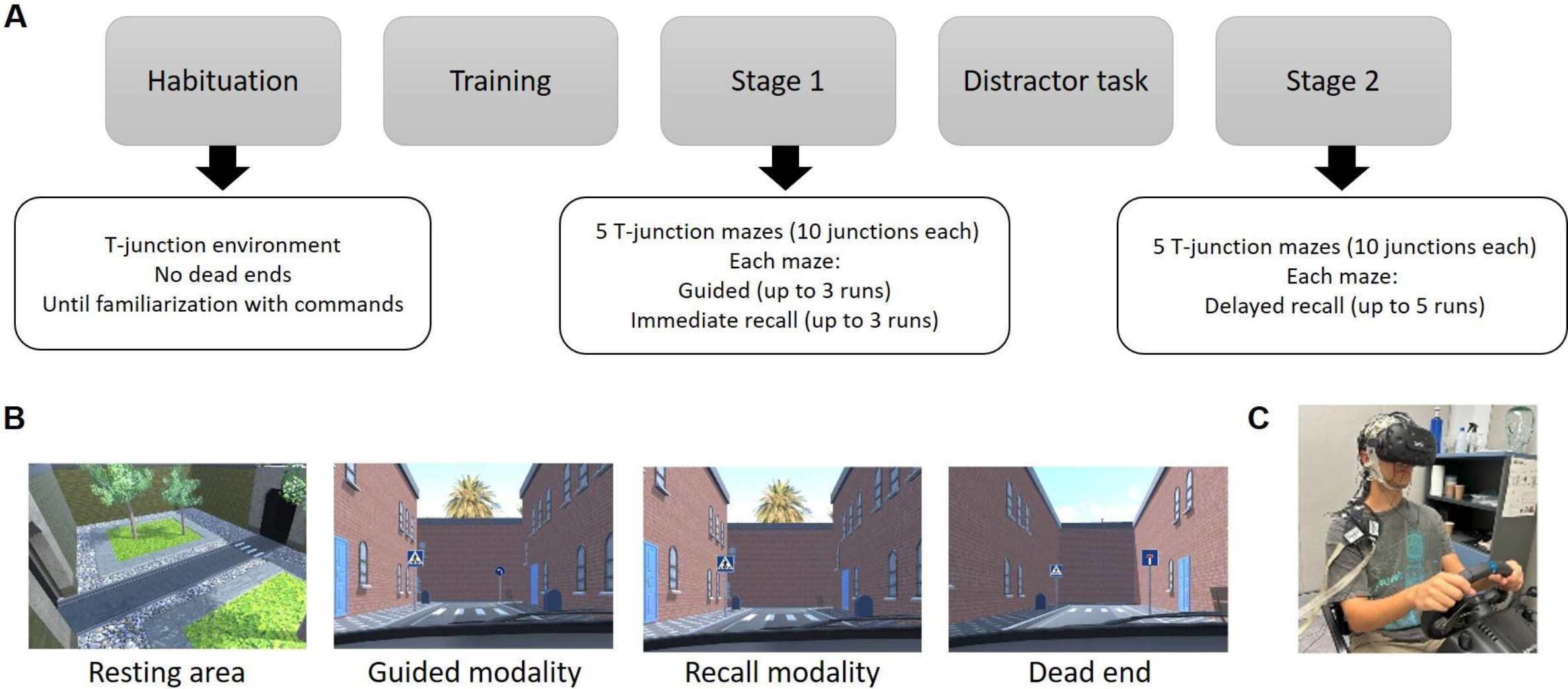
A
Habituation
Training
Stage 1
Distractor task
Stage 2
T-junction environment
No dead ends
Until familiarization with commands
5 T-junction mazes (10 junctions each)
Each maze:
Guided (up to 3 runs)
Immediate recall (up to 3 runs)
5 T-junction mazes (10 junctions each)
Each maze:
Delayed recall (up to 5 runs)
B
Resting area
Guided modality
Recall modality
Dead end
C